

The Triple-Ring Nebula around SN 1987A: Fingerprint of a Binary Merger

Thomas Morris,^{1,2} Philipp Podsiadlowski^{1,*}

¹Dept. of Astrophysics, University of Oxford, Oxford OX1 3RH, UK

²Max-Planck Institut für Astrophysik, Garching, Germany

*E-mail: podsi@astro.ox.ac.uk.

Supernova 1987A, which was the first naked-eye supernova since Kepler's supernova in 1604. It was an unusual supernova that in many respects defied theoretical expectations. It has long been suspected that these anomalies were the result of the merger of two massive stars some 20,000 years before the explosion, but so far there has been no conclusive proof. Here we present three-dimensional hydrodynamical simulations of the mass ejection associated with such a merger and the subsequent evolution of the ejecta and show that this reproduces the properties of the triple-ring nebula surrounding the supernova in all its details.

Supernova 1987A (SN 87A) in the Large Magellanic Cloud was one of the major astronomical events of the 1980s, but it was highly unusual. The progenitor star, Sk $-69^{\circ}202$, was one of the major surprises. While massive stars similar to the progenitor of SN 87A are expected to end their evolution as red supergiants, Sk $-69^{\circ}202$ was a blue supergiant. Moreover, the outer layers of the star were highly enriched in helium (1), suggesting that some nuclear processed material from the core was mixed into the envelope by a non-standard mixing process (2). Most spectacularly, the supernova is surrounded by a complex triple-ring nebula (3, 4), consisting of material that was ejected from the progenitor some 20,000 yr before the explosion in an almost axi-symmetric but in a very non-spherical manner. All of this has pointed to some dramatic event that occurred to the progenitor some 20,000 yr before the explosion, most likely the merger of two massive stars (5).

A merger was first suggested to explain some of the asymmetries of the supernova ejecta (6). Later it was realized that a binary merger can also explain the blue progenitor and the main chemical anomalies of the event (7–9). The latter was confirmed in detailed stellar, hydrodynamical simulations of the slow merger of two massive stars (10). However, the origin of the triple-ring nebula has so far not found a satisfactory explanation.

The triple-ring nebula consists of three overlapping rings in projection. The supernova occurred at the center of the inner ring, while the outer rings are in planes almost parallel to the central ring plane but displaced by 0.4 pc above and below the central ring plane. It is important to note that these outer rings do not form the limb-brightened projection of an hourglass nebula, as in some of the early models for the nebula (11–13), but dense, ring-like density enhancements (4). Previous attempts to model the nebula have involved interacting winds in a binary (14, 15), a photoionization-driven instability (16), mass ejection during a binary merger (17) or magnetically controlled ejection (18), but none of these have been able to fully explain both the detailed geometry and the kinematical properties of the nebula.

The axi-symmetric, but very non-spherical structure immediately suggests that rotation may have played a role in the formation. However, it follows from simple angular-momentum conservation arguments that any single star that is rotating rapidly in its early evolution could only be rotating slowly after it has expanded by a factor of ~ 100 to red-supergiant dimensions. On the other hand, a binary merger provides a simple and effective means of converting orbital angular momentum into spin angular momentum and of producing a single, rapidly rotating supergiant.

In a typical binary merger model for SN 87A (9), the system initially consisted of two massive stars with masses of $\sim 15 M_{\odot}$ and $\sim 5 M_{\odot}$ in a fairly wide orbit with an orbital period longer than ~ 10 yr, so that the more massive component only starts to transfer mass to its companion after it has completed helium burning in the core. Because of the large mass ratio, mass transfer is expected to be unstable and to lead to a common envelope phase, where the secondary is engulfed within the primary’s envelope (Fig. 1). In this phase, most of the orbital angular momentum of the binary is deposited in the common envelope spinning it up in the process. Because of friction with the envelope, the secondary will start to spiral-in inside the common envelope. Since the density increases inwards, the spiral-in process initially accelerates, until enough orbital energy has been released and deposited in the envelope to affect the envelope dynamically. Because the timescale of this energy ejection is comparable to the dynamical timescale of the envelope, the energy injection into the envelope is essentially impulsive leading to a dynamical expansion of the envelope and significant mass ejection. After the envelope has expanded, the spiral-in of the secondary slows down and now occurs in a self-regulated manner, where all the orbital energy released is transported to the surface, where it is radiated away. Ultimately, the secondary inside the envelope will merge with the core leading to the dredge-up of core material from the primary core (10). The whole merger process is expected to take a few 100 yr. Afterwards the star will initially be an oversized red supergiant, but will shrink in a few 1000 yr, the timescale on which the envelope loses its excess thermal energy, to become a blue supergiant. In this latter phase, the fast, energetic wind from the blue supergiant will sweep up the ejecta associated with the merger and shape the whole nebula.

To simulate the mass ejection during the merger and the subsequent evolution of the ejecta, we use GADGET (19), a three-dimensional, particle-based hydrodynamics code, using the smooth-particle hydrodynamics (SPH) method. We split the simulations into two parts. First, we simulate the mass ejection associated with the merger and then take the output from this

model to start a second calculation to simulate the subsequent evolution of the ejecta as they are being swept up by the blue-supergiant wind.

We model the red supergiant as a polytrope with a central point source of $8 M_{\odot}$, representing the compact core of the star and the immersed companion, and an envelope mass of $12 M_{\odot}$; the initial radius of the star is taken to be $1500 R_{\odot}$. We then mimic the initial spin-up phase by adding angular momentum to the envelope over a period of ~ 6 yr until all the angular momentum from the initial binary is deposited in the envelope (20). Because of this spin-up, the envelope will become highly non-spherical and take on a disk-like shape (Fig. 2a). Most of the orbital energy is injected impulsively when the orbital energy released is comparable to the binding energy of the envelope (21). This produces an inner region of overpressure which starts to expand and drive a shock in the overlying layers, ejecting some of the outer layers in the process. Because of the highly flattened envelope structure, mass ejection is easiest in the polar direction and occurs there first. Whether mass is ejected in the equatorial direction depends on the amount of energy injected. If it is less than $\sim 1/3$ the binding energy of the envelope, the large mass concentration in the equatorial plane inhibits equatorial mass ejection (20): particles that try to escape in the equatorial direction are deflected by the large equatorial mass concentration towards higher latitudes (Fig. 2c). This produces a large density enhancement in the ejecta at roughly 45 degrees. Indeed, it is the overdensity at mid-latitude that will ultimately be swept up to form the outer rings in the SN 87A nebula.

In our best model, no matter is ejected in the equatorial direction. However, because the merged object has much more angular momentum than a more compact blue supergiant could have, the merged object has to lose this excess angular momentum, most likely in the form of a slow equatorial outflow (22), as it shrinks to become a blue supergiant. We estimate that, for typical parameters, most likely several solar masses need to be lost in this transition phase (see (21) for further discussion). Once the merged object has become a blue supergiant, its energetic blue-supergiant wind will start to sweep up all the structures ejected previously.

To model the blue-supergiant phase, we start a second SPH calculation where we only simulate the ejecta. For the initial model of this calculation we take the output from the first simulation once the ejecta expand freely. This gives the mass and the velocity of the ejecta as a function of latitude. We then ballistically extrapolate the evolution of the ejecta for 4000 yr, the assumed time of the red–blue transition. We model the equatorial mass shedding by including an equatorial outflow, lasting for 2000 yr (21). We then turn on a spherically symmetric blue-supergiant wind (with a mass loss rate of $\dot{M} = 2 \times 10^{-7} M_{\odot} \text{ yr}^{-1}$ and wind velocity $v_w = 500 \text{ km s}^{-1}$) and follow the subsequent evolution.

In a typical simulation after $\sim 20,000$ yr (Fig. 2d), the density enhancement at mid-latitude has been swept up into two well-defined rings, which together with the swept-up equatorial outflow produce the main features of the triple-ring nebula when observed at an inclination of ~ 45 deg (Fig. 2e).

The HST image (4) of the nebula shows that the symmetry center of the outer rings is slightly displaced from the symmetry axis of the central ring. This asymmetry can be easily explained if the ejecta associated with the merger are given a small kick of $\sim 2 \text{ km s}^{-1}$ in a

direction to the north-west of the nebula, at an angle of 11° out of the equatorial ring plane. This was done to produce the model shown in Figure 2e, which almost perfectly reproduces not only the main features of the triple-ring nebula but also the small asymmetries of the outer rings (their deviations from perfect ellipses and their displacement from the central symmetry axis). To generate this emission model (21), we assumed that the nebula is fully ionized by the SN explosion and that the emission is optically thin. This ‘best’ model also reproduces the kinematics of both the inner ring (23) and the outer rings (4). In this particular model, the inner ring contains $0.4 M_\odot$ of mass, while the outer rings contain a total of $0.02 M_\odot$ each.

The physical origin of this small kick is not entirely clear. It could be associated with a non-radial pulsational mode excited during the early spiral-in phase; alternatively it could be due to the orbital motion caused by a more distant low-mass third star in the system.

In addition to the three rings, the model predicts several other structures. The outer rings form the ends of two bipolar lobes which combined with the bow-shock structure around the inner ring are reminiscent of an hourglass nebula (Fig. 2d). This structure is presumably the origin of the hourglass structure that has been inferred from light-echo studies (24). Further light echoes were also detected from beyond the triple-ring structure as summarised in (25); these were most likely formed during the earlier red-supergiant phase of the primary star before the merger or in the phase immediately preceding the merger, where accretion on the companion may produce a bipolar outflow (e.g. (26)), phases not included in our simulations.

The hydrodynamical model we have presented here provides an excellent fit to the observed triple-ring nebula around SN 1987A. It is important to emphasize that this model does not require any physically ad hoc assumptions and that all the input parameters are compatible with the values expected from simple modelling of the various phases of the merger (apart from the physical origin of the small kick to the ejecta, which is presently not explained).

The model also makes several predictions, specifically about the mass in the different rings and other structures. These may ultimately become visible when the nebula is being destroyed by the supernova ejecta or when the nebula is being re-ionized by the emergent X-ray flux resulting from the supernova–ring interaction. Since in our favoured model the outer rings are ejected before the dredge-up of core material, while the inner ring is ejected afterwards, one may expect some chemical differences between the inner ring and the outer rings, where the inner ring should show a larger helium enhancement and more evidence for CNO processing than the outer rings. There is the tantalizing hint that this may already have been observed (27), but this needs to be confirmed in a more detailed comparative study.

References and Notes

1. G. Sonneborn, *et al.*, *Astrophys. J.* **477**, 848 (1997)
2. H. Saio, K. Nomoto, M. Kato, *Astrophys. J.* **331**, 388–393 (1988)
3. E. J. Wampler, *et al.*, *Astrophys. J.* **362**, L13 (1990)

4. C. Burrows, *et al.*, *Astrophys. J.* **452**, 680 (1995)
5. R. McCray, *Nature* **386**, 438 (1997)
6. R. A. Chevalier, N. Soker, *Astrophys. J.* **341**, 867 (1989)
7. Ph. Podsiadlowski, P. C. Joss, S. Rappaport, *Astron. Astrophys.* **227**, L9 (1990)
8. W. Hillebrandt, F. Meyer, *Astron. Astrophys.* **219**, L3 (1989)
9. Ph. Podsiadlowski, *Publ. Astron. Soc. Pac.* **104**, 717 (1992)
10. N. Ivanova, Ph. Podsiadlowski, in *From Twilight to Highlight: the Physics of Supernovae*, W. Hillebrandt, W., B. Leibundgut, Ed. (Springer, Berlin, 2003), pp. 19 – 22
11. D. Luo, R. McCray, *Astrophys. J.* **379**, 659 (1991)
12. P. Lundqvist, C. Fransson 1991, *Astrophys. J.* **380**, 575 (1991)
13. C. Martin, D. Arnett, *Astrophys. J.* **447**, 378 (1995)
14. Ph. Podsiadlowski, A. C. Fabian, I. R. Stevens, *Nature* **354**, 43 (1991)
15. M. Lloyd, T. O'Brien, F. Kahn, *Mon. Not. R. Astron. Soc.* **273**, L19 (1995)
16. F. Meyer, *Mon. Not. R. Astron. Soc.* **285**, L11 (1997)
17. N. Soker, *Mon. Not. R. Astron. Soc.* **303**, 611 (1999)
18. T. Tanaka, H. Washimi, *Science* **296**, 321 (2002)
19. V. Springel, N. Yoshida, S. White, *New Astronomy* **6**, 51 (2001)
20. T. Morris, Ph. Podsiadlowski, *Mon. Not. R. Astron. Soc.* **365**, 2 (2006)
21. Materials and methods are available as supporting material on Science Online.
22. A. Heger, N. Langer, *Astron. Astrophys.* **334**, 210 (1998)
23. A. P. Crotts, S. R. Heathcote, *Nature* **350**, 683 (1991)
24. J. Xu, A. Crotts, W. Kunkel, *Astrophys. J.* **451**, 806 (1994)
25. B. Sugerman, A. Crotts, W. Kunkel, S. Heathcote, S. Lawrence, *Astrophys. J.* **627**, 888 (2005)
26. N. Soker, astro-ph/0610655 (2006)

27. N. Panagia, S. Scuderi, R. Gilmozzi, P. M. Challis, P. M. Garnavich, R. P. Kirshner, *Astrophys. J.* **459**, L17 (1996)
28. The authors would like to thank Prof. Lorne Nelson for providing access to the Bishop/Sherbrooke Beowulf cluster (Elix3) which was used to perform the interacting winds calculations discussed in this paper. The binary merger calculations were performed on the UK Astrophysical Fluids Facility. TM acknowledges support from the Research Training Network ‘Gamma-Ray Bursts: An Enigma and a Tool’ during part of this work.

Supporting Online Material

www.sciencemag.org

Materials and Methods

Nebula Geometry

Tables S1, S2

Movie S1, S2

Figure 1. Schematic diagram illustrating the formation of the triple-ring nebula. The system initially consisted of a binary with two stars of $\sim 15 M_{\odot}$ and $\sim 5 M_{\odot}$, respectively, with an orbital period $\gtrsim 10$ yr. (a) Mass transfer is dynamically unstable leading to the merger of the two components in a common envelope and (b) the spin-up of the envelope. (c) The release of orbital energy due to the spiral-in of the companion leads to the partial ejection of the envelope. (d) After the merging has been completed, the merged object evolves to become a blue supergiant, shedding its excess angular momentum in an equatorial outflow. In the final blue-supergiant phase, the energetic wind from the blue supergiant sweeps up all the previous structures, producing the triple-ring nebula.

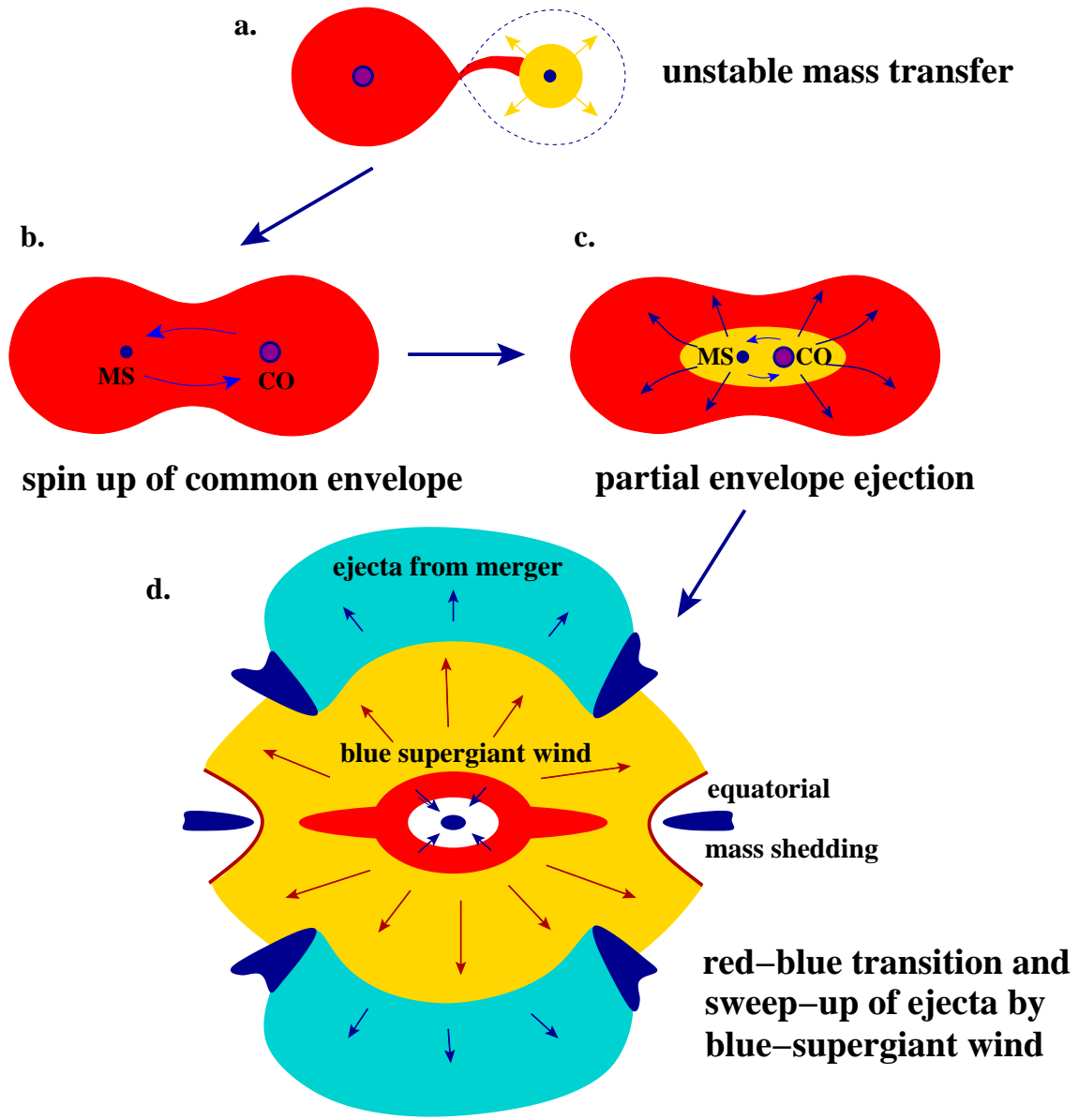
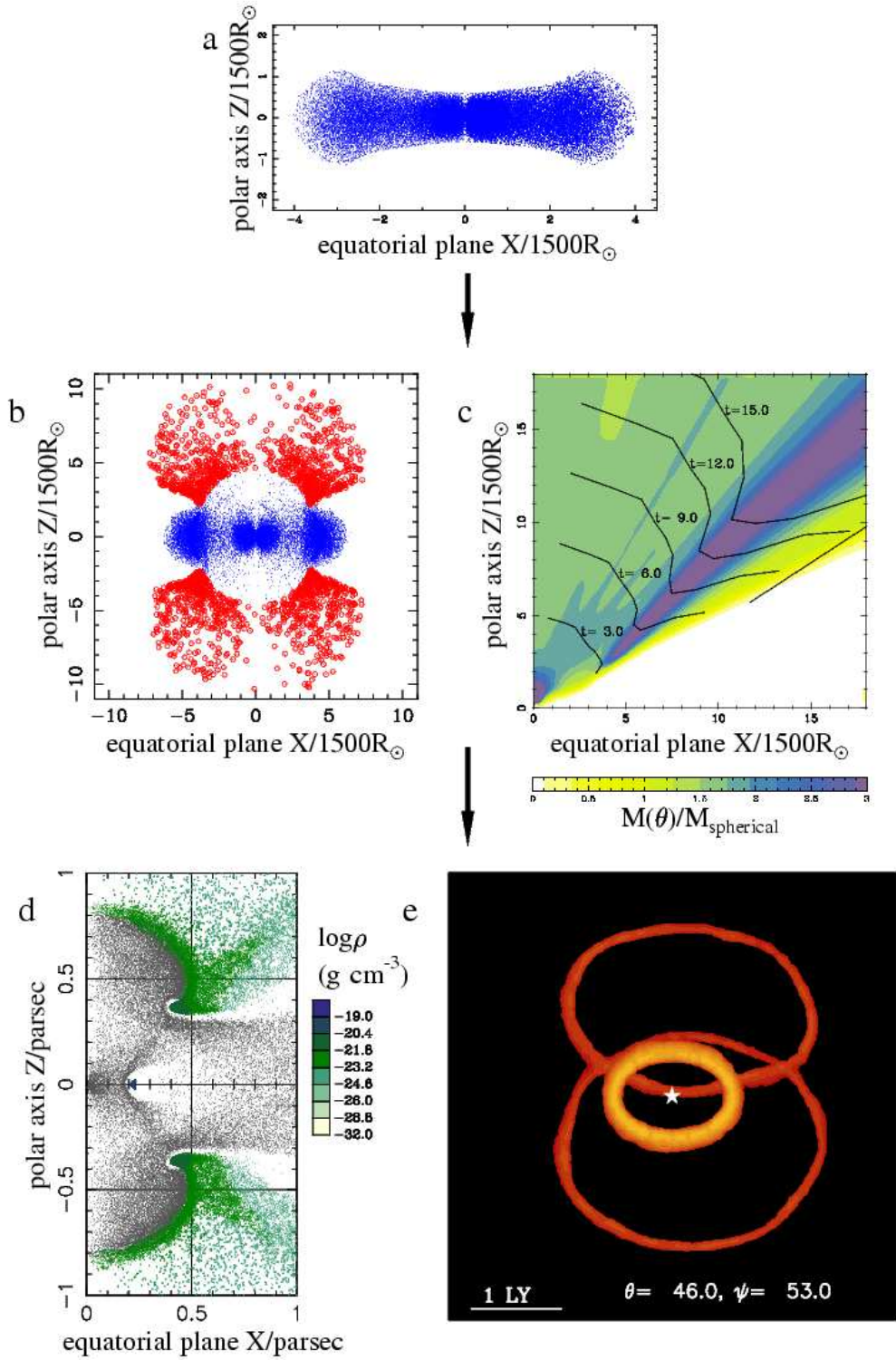


Figure 2. Three-dimensional hydrodynamical (SPH) simulations to model the various phases illustrated in Fig. 1. (a): Cross-section of the rapidly rotating red-supergiant envelope, containing 2×10^5 SPH particles, following the spin-up in the initial common-envelope phase (Fig. 1b) after a total amount of orbital angular momentum of $L = 8 \times 10^{54}$ erg s has been deposited in the envelope. In these units, the red supergiant had an initial radius of 1. (b): Particle snapshot in the meridional plane approximately 3 yr after the orbital energy has been injected in the central part of the common envelope (cf. Fig. 1c), showing the formation of the enhancement at mid-latitudes. Red particles are unbound. (c): The mass enhancement in the ejecta plotted as a function of time (contours) and distance from the centre of mass, as a function of latitude. The horizontal axis shows the equatorial plane where no mass is ejected, and the colour scale beneath the plot shows the increase of ejected mass over the value expected in spherical symmetry. The contours show the mean radius of the ejected material at the time shown, in units of 0.8 yr ($2I$). The axes are in the same unit system as those of (a) and (b). (d): The final particle distribution (10^6 particles) plotted in the meridional plane at an age of 20 kyr. The density and mean velocity of the material in the equatorial ring (outer rings) is $\sim 2 \times 10^4 \text{ cm}^{-3}$ (10^3 cm^{-3}) and 10.3 km s^{-1} (31 km s^{-1}), respectively. Wind particles are shown in black while the nebula particles are shown in dark blue through pale green based on a logarithmic density scale as indicated (in CGS units). The axes are in units of $3 \times 10^{18} \text{ cm}$. (e): Simulated emission measure at $\sim 2000 \text{ d}$ after the supernova in the $656 \text{ nm H}\alpha$ line for our ‘best’ model. The total flux from the outer rings is $4 \times 10^{45} \text{ photons s}^{-1}$, comparable to the observed flux (4).



Materials and Methods

Binary merger phase

All hydrodynamical simulations were performed with a modified version of the publicly available GADGET code (*S1*), which uses the smooth-particle-hydrodynamics (SPH) method (*S2*) to simulate hydrodynamical flows of arbitrary geometry in three dimensions.

At the onset of the common envelope phase, the primary star is an evolved red supergiant which we approximate as a polytrope with polytropic index $n = 3/2$ containing a centrally condensed core of $M \approx 2/5M_*$. The spherically symmetric (non-rotating) density profile is sampled with 2×10^5 particles using a Monte-Carlo technique which are then relaxed using the method of Lucy (*S3*) to reduce particle noise. An adiabatic equation of state $\gamma = 5/3$ is used throughout, except for the relaxation phase for which constant entropy $s \propto p/\rho^\gamma$ is assumed (p and ρ are the pressure and density, respectively). The envelope contains significant mass at large radii and is therefore able to store a large fraction of the available orbital angular momentum

$$L_{\text{orb}} = 6.60 \times 10^{54} \text{ g cm}^2 \text{ s}^{-1} A_{2500}^{1/2} M_{15} M_5 M_{20}^{-1/2}, \quad (1)$$

which is transferred to the envelope during the early spiral-in of the companion. Here A_{2500} is the orbital separation in units of $2500 R_\odot$, M_{15} and M_5 are the masses of the primary and the secondary in units of $15 M_\odot$ and $5 M_\odot$ (as indicated by the subscripts), respectively, and $M_{20} = M_1 + M_2$ is the total mass in units of $20 M_\odot$. Previous one-dimensional calculations including energy and angular momentum transport (*S4*, *S5*) suggest that most angular momentum is deposited in the early spiral-in phase.

In our model, the angular momentum is added to the envelope slightly more slowly than the sound-crossing time of the envelope in such a manner that the particles remain sub-Keplerian at all times. The gain in angular velocity on each particle is given by

$$\Delta\Omega = \begin{cases} \gamma\Delta t & \text{if } v_i/v_{\text{Kepler}} < 1 \text{ always,} \\ 0 & \text{otherwise} \end{cases} \quad (2)$$

which leads to a stable angular momentum profile with a core rotating close to the local Keplerian velocity at each cylindrical radius, and an extended envelope with a constant specific angular momentum profile (see Fig. 1 of *S6*).

The energy deposited in the envelope corresponds to the orbital energy lost by the companion during the plunge-in phase when its orbit decreases from $r \sim 1R_*$ to $r \sim 0.1R_*$. The available energy is roughly (also see table S1)

$$\Delta E_{\text{orb}} = 5.0 \times 10^{46} \text{ erg } M_{10} M_2 (R_i/R_f - 1), \quad (3)$$

where M_{10} and M_2 are the primary and secondary masses at a separation of $\sim 1/5R_*$ in units of 10 and 2 solar masses, respectively, and R_i and R_f are the initial and final orbital separation. Most of this energy is deposited in the inner envelope, corresponding to 1.5×10^{47} erg in the

merger model discussed in this paper, or half of the available orbital energy. The deposited energy is added to the central region $r < 200 R_\odot$ which contains $0.7 M_\odot$, corresponding to a temperature of 9×10^5 K. We have tested that the exact details of the energy deposition does not strongly affect the amount of mass in the ejecta and their geometry (also see (S6)).

The latitude-dependence of the outflowing material is illustrated in Fig. 2c in the paper. The image shows the mass enhancement ratio $M(r, \theta)/M_{\text{spherical}}$ where $M(r, \theta)$ is the ejected mass in a spherical coordinate system, divided by the spherically symmetric value $M_{\text{spherical}}$. The horizontal axis lies in the equatorial plane while the vertical axis lies along the polar direction. The contours show the median radius $r(t)$ of the ejected material at a given time t (labelled) in units of 0.8 yr, as a function of latitude, showing that the highest velocity material is ejected in the polar direction. The mid-latitude enhancement (coloured purple) corresponds to a local velocity minimum, and no material is ejected in the equatorial plane (white, $M(r, \theta)/M_{\text{spherical}} < 0.2$).

The blue loop

Following the merger, the star contracts by a factor $\gtrsim 10$ in radius and becomes a blue supergiant, on a timescale of a few thousand years. The stellar wind of the star changes from a slow dense outflow ($v_w \sim 30 \text{ km s}^{-1}$) to a much faster wind ($v_w \sim 500 - 800 \text{ km s}^{-1}$) which compresses the dense gas ejected during the binary merger. Typically 10 per-cent of the envelope is ejected, containing 2×10^4 particles which are resampled to increase the resolution to $\sim 10^6$ particles, preserving the density enhancement at mid-latitudes. These new particles are integrated on ballistic trajectories for 4 kyr to set the initial gas distribution at the beginning of the blue-supergiant phase.

The equatorial outflow occurs as the envelope loses angular momentum during the blue loop. The total mass lost can be estimated from angular momentum conservation

$$M_{ER} = \frac{\Delta L}{\sqrt{GM_\star R_\star(1 - \Gamma)}} \sim 4 M_\odot \quad (4)$$

if the mass is lost near critical rotation (as suggested by the low expansion velocity of the ring of around 10.3 km s^{-1}). Here ΔL is the excess angular momentum that needs to be lost, i.e. is the difference between the post-merger angular momentum in the envelope and the maximum angular momentum for a stable blue supergiant ($\sim 4 \times 10^{54} \text{ erg s}$). We assume an Eddington factor of $\Gamma = 0.4$ and that the envelope must lose $\sim 6 \times 10^{54} \text{ erg s}$ at a radius of roughly $6000 R_\odot$. This is likely to be a lower limit unless magnetic processes in the excretion disk can increase the specific angular momentum of material at larger radii.

We model the equatorial mass shedding by including an outflow, lasting for 2000 yr, with an assumed angular density profile $\rho \propto \cos^2(\pi\theta/2\theta_0)$ ($|\theta| \leq \theta_0$, where θ is the angle relative to the equatorial plane and θ_0 is typically 5 degrees) and the ring contains of order $0.5 M_\odot$.

We note that, while the existence of the inner ring is important for the shaping of the outer rings (see the bow shock near the inner ring in Fig. 2d), the shape of the outer rings is not sensitive to the amount of mass or the detailed geometry of the equatorial outflow.

Nebular phase

During the final blue supergiant phase, the supersonic stellar wind sweeps up the pre-existing material. In order to model this phase, we have modified the GADGET code to include the addition of new gas particles at small radii, relative to the shell, to represent the fast wind. The acceleration of these wind particles can be neglected since their initial radius r_0 is much larger than the typical stellar radius: $r_0 \sim 10^{-3} \text{ pc} \sim 10^3 R_\star$.

At each interval δt which is small relative to the crossing time of the free wind region, new particles are distributed in a sphere with radius $v_w \delta t$ where $v_w = 500 \text{ km s}^{-1}$ is the terminal velocity of the blue supergiant wind. The radial profile follows r^{-2} in the free wind region. A fixed number of particles (typically $N_w \sim 500$) are introduced, with equal masses calculated from the stellar mass-loss rate, which is assumed constant throughout the duration of the blue supergiant phase:

$$N_w m_w = \dot{M} \delta t \quad (5)$$

These are treated as gas particles in the smoothed particle hydrodynamics-based code. The code has been verified against the semi-analytic solution in the case of an adiabatic bubble in a constant density medium (S7).

Flash ionization by the supernova explosion

In order to compare our results to the HST image we simulate the $\text{H}\alpha$ emission from the nebula by integrating the square of the density along the line of sight. The relative pixel intensity is simply $\int n_e n_{\text{H}^+} dl = \int n_{\text{H}}^2 dl$ if the entire nebula is initially ionized. A simple recombination model is included with the form $n_{\text{H}^+}(t) = n_{\text{H}}(0) \exp(-\alpha n_{\text{H}} t)$ where n_{H} and n_{H^+} are the total hydrogen density and proton density, respectively, and $\alpha_B \approx 3 \times 10^{-13} \text{ cm}^3 \text{ s}^{-1}$ is the hydrogen recombination coefficient to levels $n \geq 2$. For simplicity we assume $n_e = n_{\text{H}^+}$ at all times. The pixel intensity due to a narrow ring or filament of dense material is thus

$$I \propto n_{\text{H}^+}^2 \Delta r, \quad (6)$$

which gives $I \sim 5 \times 10^{24} \text{ cm}^{-5}$ for the equatorial ring and $I \sim 2 - 5 \times 10^{22} \text{ cm}^{-5}$ for the outer rings. Pixels below a threshold intensity of $I = 2 \times 10^{21} \text{ cm}^{-5}$ along the line of sight are set to zero intensity. The equatorial ring is probably only ionized to a skin-depth of around $\sim 4 - 10 \times 10^{15} \text{ cm}$ (S8) while the rest of the ring remains neutral. The hydrogen (and much of the helium) in the outer rings is expected to be completely ionized by the supernova outburst. The density in the outer rings is found to be 100 to 150 times the density in the shocked blue-supergiant wind bubble and is a factor of 5 to 10 larger than the density in the polar lobes, accounting for the sharp appearance of the outer rings.

Supporting Text

Nebula geometry

The latitude of the outer rings is determined primarily by the location of the mass peak in the merger ejecta. The ratio of the radius of the equatorial ring to that of the outer loops is determined firstly by their velocities of ejection, which are unconstrained in the model, and secondly by their relative masses. Values of 2.5–3.5 are typical for model parameters applicable to SN 1987A (table S2).

Supporting Tables

Table 1: Selected properties of the polytope model before the spin-up/spiral-in phase (left column) and after the addition of $L = 8 \times 10^{54}$ erg s of angular momentum (right column).

Property	Before spin-up	After spin-up
Potential energy $W/10^{47}$ erg	-12.0	-7.2
Kinetic energy $T/10^{47}$ erg	0	1.1
Binding energy/ 10^{47} erg	-6.2	-4.5
Ratio T/W	0	0.15
Angular momentum $L/10^{54}$ erg s	0	8.0
Moment of inertia $I/10^{61}$ g cm ²	4.1	73.6

Table 2: Values of the radius ratio of the outer rings to the equatorial ring, for representative SN 1987A nebula calculations at an age of 22 kyr after the onset of the blue-supergiant wind. The units of the initial equatorial ring velocity $v_{ER,0}$, mass M_{ER} and wind mass-loss rate \dot{M} are km s⁻¹, M_{\odot} and $10^{-7} M_{\odot}$ yr⁻¹, respectively.

Model	$v_{ER,0}$	M_{ER}	\dot{M}	r_{NOR}/r_{ER}	r_{SOR}/r_{ER}
M1	8.0	0.4	2.0	2.79	2.86
M2	8.5	0.4	2.0	2.58	2.65
M3	9.0	0.4	2.0	2.38	2.44
M4	8.0	0.6	2.0	3.03	3.08
M5	8.0	0.8	2.0	3.09	3.13
M6	8.0	1.0	2.0	3.15	3.17
M7	8.0	1.0	2.5	3.27	3.32
M8	8.0	1.0	3.0	3.38	3.41

Movies

Movie S1: Mpeg movie showing the simulation of the mass ejection during the merger phase. Left panel: particle plot showing particles that are ejected in red and particles that remain bound in blue. The scale is in units of $1500 R_{\odot}$. Right panel: Histogram of the mass (left axis) ejected as a function of $\sin \theta$, where θ is the angle with respect to the equatorial plane. The thin blue curves give the median velocity (central curve) and the range of velocities (upper and lower curves) that includes 50 % of the ejecta at a given $\sin \theta$. The velocities are given on the right axis.

Movie S2: Mpeg movie showing the formation of the triple-ring nebula as a result of the interaction of the blue-supergiant wind (grey particles) with the matter ejected in the merger phase (green/blue particles). The colour of the ejecta particles indicates the logarithm of the mass density in units of g cm^{-3} (see scale bar). The spatial scale is in units of pc.

References and Notes

- S1. V. Springel, N. Yoshida, S. White, *New Astronomy* **6**, 51 (2001)
- S2. J. J. Monaghan, *Ann. Rev. Astron. Astrophys.* **30**, 543 (1992)
- S3. L. Lucy, *AJ* **82**, 1013 (1977).
- S4. Ph. Podsiadlowksi, *Evolution of Binary and Multiple Star Systems.*, Ph. Podsiadlowski, S. Rappaport, A. King, F. D'Antona, L. Burderi, eds. (PASP, San Francisco, 2001), p. 239.
- S5. N. Ivanova, Ph. Podsiadlowski, *From Twilight to Highlight: The Physics of Supernovae.*, W. Hillebrandt, B. Leibundgut, eds. (Springer, Berlin, 2003), p. 19.
- S6. T. Morris, Ph. Podsiadlowski, *MNRAS* **365**, 2 (2006).
- S7. J. Castor, R. McCray, R. Weaver, *ApJL* **200**, L107 (1975).
- S8. P. Plait, P. Lundqvist, R. Chevalier, R. Kirshner, *ApJ* **439**, 730 (1995).